Pharmaceutical Research, Vol. 22, No. 12, December 2005 (© 2005)
DOI: 10.1007/s11095-005-7782-y

Research Paper

Self-Assembled Biodegradable Nanoparticles Developed by Direct Dialysis for the Delivery of Paclitaxel

Jingwei Xie[1] and Chi-Hwa Wang[1,2,3]

Received June 1, 2005; accepted August 4, 2005

Purpose. The main objective of this study was to obtain self-assembled biodegradable nanoparticles by a direct dialysis method for the delivery of anticancer drug. The *in vitro* cellular particle uptake and cytotoxicity to C6 glioma cell line were investigated.
Methods. Self-assembled anticancer drugs—paclitaxel-loaded poly(D,L-lactic-co-glycolic acid) (PLGA) and poly(L-lactic acid) (PLA) nanoparticles—were achieved by direct dialysis. The physical and chemical properties of nanoparticles were characterized by various state-of-the-art techniques. The encapsulation efficiency and *in vitro* release profile were measured by high-performance liquid chromatography. Particle cellular uptake was studied using confocal microscopy, microplate reader, and flow cytometry. In addition, the cytotoxicity of this drug delivery system was evaluated using 3-(4,5-dimethylthiazol-2-yl)-2,5-diphenyltetrazolium bromide (MTT) assay on C6 glioma cell line to predict the possible dose response of paclitaxel-loaded PLGA and PLA nanoparticles.
Results. PLGA and PLA nanoparticles with or without vitamin E tocopherol polyethylene glycol succinate (TPGS) as an additive were obtained, in which the sustained release of paclitaxel of more than 20 days was achieved. The coumarin6-loaded PLGA and PLA nanoparticles could penetrate the C6 glioma cell membrane and be internalized. The cytotoxicity of paclitaxel-loaded nanoparticles seemed to be higher than that of commercial Taxol® after 3 days incubation when paclitaxel concentrations were 10 and 20 μg/ml.
Conclusions. Direct dialysis could be employed to achieve paclitaxel-loaded PLGA and PLA nanoparticles, which could be internalized by C6 glioma cells and enhance the cytotoxicity of paclitaxel because of its penetration to the cytoplasm and sustained release property.

KEY WORDS: cellular uptake; cytotoxicity; dialysis; nanoparticle; paclitaxel.

INTRODUCTION

Paclitaxel is FDA-approved for clinical use in ovarian (1) and breast cancer (2). It has shown cytotoxic activity against common solid tumors and a number of leukemias, Walker 256 carcinosarcomas, lung tumors (3), and human hepatocellular carcinoma cell lines (4). Paclitaxel is a potent inhibitor of cell replication that works by blocking cells in the late G2 or M phase of the cell cycle (5,6) and binding to cellular microtubules for promoting the polymerization of microtubules (7). In addition, it was reported that Taxol®, a tubulin drug with higher specificity for β_{II}-tubulin than for other β-tubulin isotypes, irreversibly decreases nuclear β_{II}-tubulin content in a concentration-dependent manner in C6 glioma cells (8). However, there were two main problems in the applications of paclitaxel. One is supply and the other is formulation. The problem of supply has been resolved by means of semisynthetic approaches based on the taxane skeleton, which is widely available from more abundant relatives of the Pacific Yew. More recently, developments in plant biotechnology have enabled the use of plant tissue culture to produce relatively large amounts of paclitaxel in a controlled bioreactor, thus protecting the environment by reducing the need to cut down more trees (9). The problem of formulating paclitaxel, however, still remains a large obstacle because of the widespread use of the drug. Paclitaxel is currently administered in a vehicle formulation composed of 1:1 blend of Cremophor EL (polyethoxylated castor oil) and ethanol, which is diluted with 5- to 20-fold in normal saline or dextrose solution (5%) for administration. This formulation is stable in unopened vials for 5 years at 4°C. However, there are lots of problems employing this vehicle (10,11). This is mainly because Cremophor EL has a number of associated side effects including hypersensitivity reactions, nephrotoxicity, neurotoxicity, and cardiotoxicity. Because of

[1] Department of Chemical and Biomolecular Engineering, National University of Singapore, 4 Engineering Drive 4, Singapore 117576, Singapore.
[2] Molecular Engineering of Biological and Chemical Systems, Singapore-MIT Alliance, Singapore 117576, Singapore.
[3] To whom correspondence should be addressed. (e-mail: chewch@nus.edu.sg)

ABBREVIATIONS: DMF, dimethylformamide; PBS, phosphate-buffered saline; PLA, poly(poly(L-lactic acid); PLGA, poly(D,L-lactic-co-glycolic acid).

the many problems associated with the current formulation of paclitaxel, novel drug delivery device systems will be developed in this study. Nanoparticulate carriers could be an ideal solution for intravenous injection delivery of paclitaxel and other central nervous system drugs (12). The use of polymeric particles has shown to be promising in cancer chemotherapy (13,14). Nanoparticles have been prepared mainly by two methods: (1) dispersion of the performed polymers, such as solvent evaporation method (15), spontaneous emulsification/solvent diffusion method (16), nanoprecipitation method (17–19), supercritical fluid technology, etc.; and (2) polymerization of monomers (20,21). Commonly, emulsion solvent evaporation method is widely employed for the preparation of nanoparticles. In this method, large amounts of emulsifiers are required to stabilize the dispersed oil droplets. In particular, polyvinyl alcohol (PVA) is most frequently used as a stabilizing emulsifier to fabricate nanoparticles. However, PVA has some problems in that it remains at the surface of the nanoparticles and is difficult to remove subsequently. It is known that PVA existing on the surface of nanoparticles changes biodegradability, biodistribution, particle cellular uptake, and drug-release behavior (22,23). Recently, dialysis method was developed for the simple preparation of drug carriers such as liposomes and polymeric micelles (24). However, little work has been performed to fabricate nanoparticles using direct dialysis methods (25,26). The objective of this work was to develop the biodegradable PLGA and PLA polymeric nanoparticulate drug delivery system by direct dialysis. Furthermore, *in vitro* experiments (paclitaxel *in vitro* release, particle cellular uptake, and particle cytotoxicity) were performed to study drug transport, particle uptake efficiency, and to evaluate the cytotoxicity of this dosage form using C6 glioma cell line. The formulations generated from this work may be considered for intratumoral or intravenous injection administration of paclitaxel.

MATERIALS AND METHODS

Materials

Paclitaxel used in the present study was purchased from Dabur India (Uttar Pradesh, India). Polymers such as poly(D,L-lactic-co-glycolic acid) (PLGA) with L/G molar ratio of 50:50 (MW = 90,000–120,000) and poly(L-lactic acid) (PLA; MW = 85,000–160,000) were purchased from Sigma Aldrich (St. Louis, MO, USA). Vitamin E tocopherol polyethylene glycol succinate (TPGS) was purchased from Eastman Chemical Company (Kingsport, TN, USA). Phosphate-buffered saline (PBS) buffer used for *in vitro* release study was bought from Sigma Aldrich containing 0.1 M sodium phosphate and 0.15 M sodium chloride, pH 7.4. Commercial Spectro/Por® membrane (molecular weight cutoff: 3500) was bought from Spectrum Laboratories Inc. (Rancho Dominquez, CA, USA). Propidium iodide (PI) and coumarin6 were obtained from Molecular Probes and Polysciences Inc. (Warrington, PA, USA), respectively. Dimethylformamide (DMF) and acetonitrile of high-performance liquid chromatography (HPLC)/Spectro grade were acquired from Tedia (Fairfield, OH, USA). All other materials and reagents used were of analytical grade.

Preparation of Nanoparticles

Amounts of 10–1000 mg of polymer and paclitaxel (10% or 5%) with and without vitamin E TPGS (5%) as an additive were dissolved in 10 ml of DMF. The resulting solution, with the organic phase, was subsequently loaded into the dialysis membrane. Following this, the dialysis membrane was placed into the external aqueous phase of water. The organic solvent diffused out of the membrane, leading to precipitation and separation of the polymer molecules out of solvent to gather and self-assemble to form spherical nanoparticles. The external water phase was gently stirred using a magnetic stirrer to aid diffusion. The organic phase was dialyzed against the aqueous phase for 24 h, with changes of the aqueous phase every 2–3 h until the organic solvent had been completely removed by diffusing out of the dialysis membrane. Then, the sample solution in the membrane was collected and centrifuged at 11,500 rpm for 30 min in Eppendorf Centrifuge 5810R. The nanoparticles were obtained as the pellet and further freeze-dried.

Morphology of Nanoparticles

The morphology of nanoparticles was observed using scanning electron microscopy (SEM). SEM (Jeol JSM 5600LV) requires an ion coating with platinum by a sputter coater (JFC-1300, Jeol, Tokyo) for 40 s in a vacuum at a current intensity of 40 mA after preparing the sample on metallic studs with double-sided conductive tape. The accelerating voltage ranged from 5 to 15 mV during scanning.

Drug Physical Status Characterization

This characterization was performed by jointly measuring the differential scanning calorimetry (DSC) and X-ray diffractometry (XRD) patterns. To carry out DSC tests, 8 mg of sample was sealed in standard aluminum pans with lids. The sample was purged with pure dry nitrogen at a flow rate of 20 ml/min. The temperature ramp speed was set at 10°C/min, and the heat flow was recorded from 0 to 250°C. Indium was used as the standard reference material to calibrate the temperature and energy scales of the DSC instrument. The X-ray powder diffraction patterns for pure paclitaxel and different drug loading samples were obtained with a model XRD-2000 X-ray powder diffractometer, Rigaku (Tokyo, Japan). The measurements were performed in the 2–40° 2θ range at a rate of 2° 2θ/min using CuKα radiation (45 kV, 40 mA) as X-ray source.

Zeta Potential Analysis

Particles (1.5 mg) were suspended in 1.5 ml KCl solution (1 mM); the suspension was loaded into an optical well and detected by Zeta Potential analyzer (Zeta Plus, Brookhaven Instruments, Holtsville, NY, USA). A higher zeta potential value indicates more negative charges on the surface of particles and hence more stable particle suspension could be obtained. Under such conditions, particles are less likely to aggregate and form flocculation or coagulation and can be well suspended in water-based solution. Well-suspended

particles may be taken up by cells more easily than aggregated ones.

In Vitro Paclitaxel Release Studies

Nanoparticles (10 mg) were dispersed in 10 ml of PBS (pH 7.4) containing 1% of Tween 80 to enhance the solubility of paclitaxel. The buffer solution was kept at constant temperature of 37.2°C. At given time intervals, three tubes of each formulation of nanoparticles were withdrawn and centrifuged at 11,500 rpm for 10 min. The precipitated nanoparticles were taken and resuspended in 10 ml of fresh release medium and placed back in the shaker. The supernatant solution was retained for HPLC analysis. Paclitaxel in the release medium was first extracted with 1 ml of dichloromethane (DCM). A mixture of acetonitrile and water (50:50 v/v) was added to the extracted paclitaxel after the DCM had evaporated. The resulting solution was analyzed using HPLC, in which C-18 column was used and the mobile phase was delivered at a rate of 1 ml/min. One hundred microliters of sample was injected by an autosampler, and the column effluent was detected at 227 nm using an ultraviolet (UV) detector. The data from detection were corrected according to the extraction efficiency.

Cell Culture

C6 glioma cells (courtesy of Singapore General Hospital, passages 6–10) were grown and routinely maintained at 37°C in 75-cm^2 culture flasks, in Dulbecco's Modified Eagle Medium (DMEM) supplemented with 10% fetal calf serum, 1% penicillin–streptomycin in atmosphere of 5% CO_2, and 90% relative humidity. The cells were harvested with trypsin–ethylenediaminetetraacetic acid. Medium was changed every other day.

Particle Cellular Uptake Studies

For the cell uptake experiment, the cells were seeded in the 96-well plate (black) incubated with coumarin6-loaded particle suspension (250, 500, and 1000 μg/ml in medium, pH 7.4). The particle cellular uptake efficiency of particles was determined by a microplate reader (GENios, Groedig, Austria). Cells were transferred to 96-well plate first to ensure 1×10^4 cells per well. Medium was changed every other day until 80% confluence was reached. The medium was then replaced with 100-μl medium with coumarin6-loaded nanoparticles of different concentrations. The plate was incubated for 1 or 2 h. For each type of particles, one control was kept by adding particle solution in the well. At different time intervals, suspension was removed and the wells were washed three times using PBS. After adding 100 μl 0.5% triton X-100 in NaOH to break the cells, the plate was measured using a microplate reader. The excitation wavelength and emission wavelength was 430 and 485 nm, respectively, for coumarin6. As the coumarin6 was assumed dispersed evenly in particles, the amount of particles was assumed to be linearly proportional to the microplate readings. The cellular uptake efficiency was given by the ratio between the amount of particles taken up in cells and the amount of those in control. For confocal microscopy experiment, C6 glioma cells were incubated in 4-well glass slides. After 80% confluence was reached in each well, the medium was replaced with 400-μl particle suspension (250 μg/ml). After incubation for 1 or 2 h, the suspension was removed and 10 μl of 70% ethanol solution was added into each well to fix cells. Cells with ethanol solution were kept in 37°C for 20 min, then ethanol solution was removed and PBS was used to wash wells for three times; subsequently, 10 μl (5 mg/ml) propidium iodide (PI) was added to stain cell nucleolus for 30–40 min. After PI was washed three times using PBS, the 4-well glass slides was observed by confocal laser scanning microscopy (Zeiss LSM 410) using Fluoview FV300 software. Coumarin6-loaded particles and PI-staining cell nucleus showed green color and red color, respectively. For flow cytometry experiment, C6 glioma cells were cultured in T25 culture flask till 80% confluence. Coumarin6-labeled PLGA nanoparticles (250 μg/ml) were incubated with C6 glioma cells. At different time intervals, the cells were washed with cold PBS three times. The cells were harvested using trypsin and fixed by 1% of paraformaldehyde PBS solution. Finally, the cells were measured by flow cytometry.

Cytotoxicity Studies

The cell viability was determined by a microplate reader (GENios). Cells were transferred to 96-well plate first to ensure 1×10^4 cells per well. Medium was changed every other day until 80% confluence was reached. Then the medium was changed with 100-μl medium with paclitaxel-loaded nanoparticles of different concentrations. The plate was incubated for 1, 2, and 3 days. One row of 96-well plates was used as control without adding nanoparticles. At different intervals, suspension was removed and the wells were washed three times using PBS. Ten microliters of 3-(4,5-dimethylthiazol-2-yl)-2,5-diphenyltetrazolium bromide (MTT) assay and 90 μl of medium were then added to the wells. After incubation for around 3–4 h, solution was removed, leaving the precipitate. One hundred microliters of isopropanol or DMSO was then added to the wells before the plate was observed using microplate reader. Cell viability was determined by

$$\text{Cell viability}\,(\%) = (\text{Abs test cells}/\text{Abs control cells}) \times 100 \quad (1)$$

where Abs test cells and Abs control cells represent the amount of formazan determined for cells treated with the different formulations and for control cells (nontreated), respectively (18).

RESULTS AND DISCUSSION

Surface Morphology and Particle Size

The morphology of paclitaxel-loaded and coumarin6-loaded nanoparticles fabricated by dialysis method was examined by SEM, which was shown in Fig. 1. The nanoparticles appeared to be spherical in shape and the surface was smooth. The mean size of PLGA and PLA nanoparticles obtained in this study is about 300 nm, which was measured

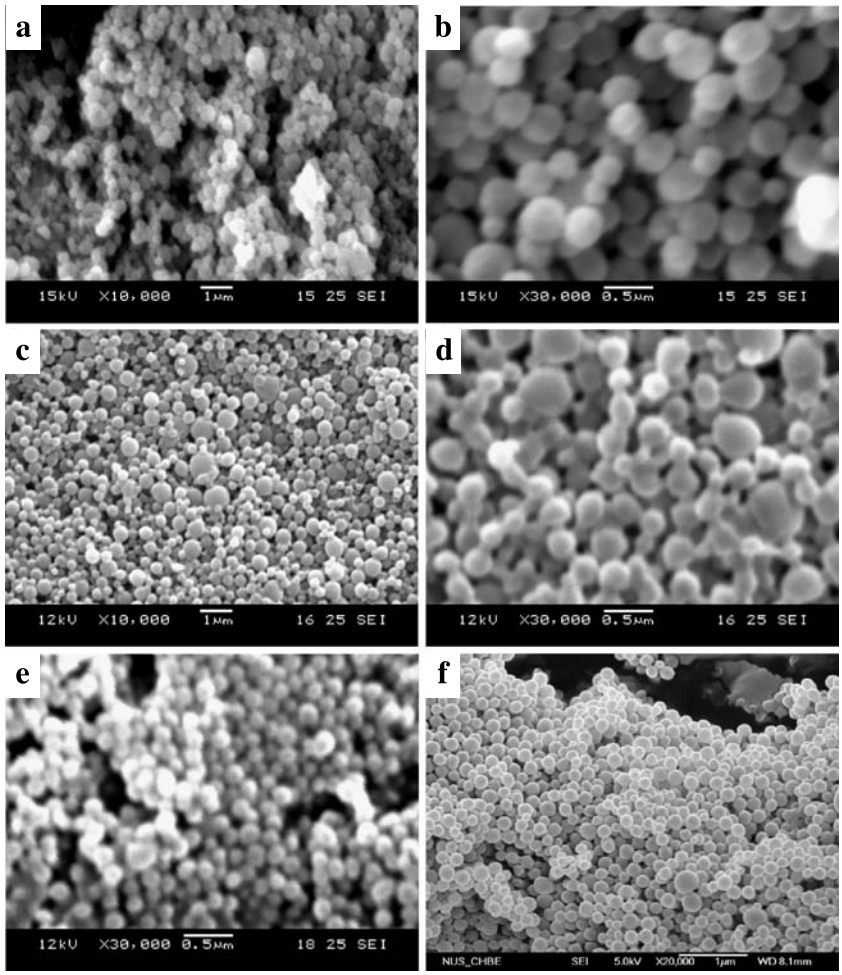

Fig. 1. Scanning electron microscopy (SEM) images of paclitaxel-loaded polymeric nanoparticles. (a, b) Paclitaxel-loaded poly(D,L-lactic-co-glycolic acid) (PLGA) nanoparticles; (c, d) paclitaxel-loaded poly(L-lactic acid) (PLA) nanoparticles; (e) coumarin6-labeled PLGA nanoparticles; (f) coumarin6-labeled PLA nanoparticles.

by laser scattering analysis (shown in Table I). In the fabrication process, the controllable particle size from 200 to 1000 nm could be achieved by adjusting the polymer concentration. In addition, pure paclitaxel and different drug-loading PLGA particles were observed by SEM, which indicated that some paclitaxel could not be encapsulated in the polymer matrix in higher drug-loading samples (30 and 20%; as shown in Fig. 2).

Table I. Particle Characterization[a]

Sample	Encapsulation efficiency (%)	Drug loading (%)	Particle size (nm)
S1	57.9	5.7	310 ± 28
S2	58.9	5.7	291 ± 32
S3	75.9	4.2	280 ± 28
S4	90.1	2.0	290 ± 25
S5	69.0	4.1	286 ± 10

S1: Paclitaxel-loaded PLA nanoparticles; S2: paclitaxel-loaded PLGA nanoparticles; S3: paclitaxel-loaded PLGA nanoparticles, vitamin E TPGS (5%) as an additive in the fabrication progress; S4: paclitaxel-loaded PLGA nanoparticles, vitamin E TPGS (5%) as an additive in the fabrication process; S5: paclitaxel-loaded PLGA nanoparticles.

[a] Each data point shown is the average of three samples.

Drug Physical Status Characterization

Figure 3 shows the DSC thermogram analysis, which provided qualitative and quantitative information about the physical status of the drug in the nanoparticles. The drug loading of the samples in DSC experiment is about 5.7%. The pure paclitaxel shows an endothermic peak of melting at 223.0°C. There was no peak observed at the temperature range of 150–250°C for the samples. The DSC study did not detect any crystalline drug material in the nanoparticle samples. It could thus be concluded that the paclitaxel formulated in the samples was in an amorphous or disordered-crystalline phase of a molecular dispersion or a solid solution state in the polymer matrix after fabrication. Moreover, the glass transition temperature of the polymers employed in paclitaxel-loaded PLGA and PLA nanoparticles was obviously not influenced by the procedure.

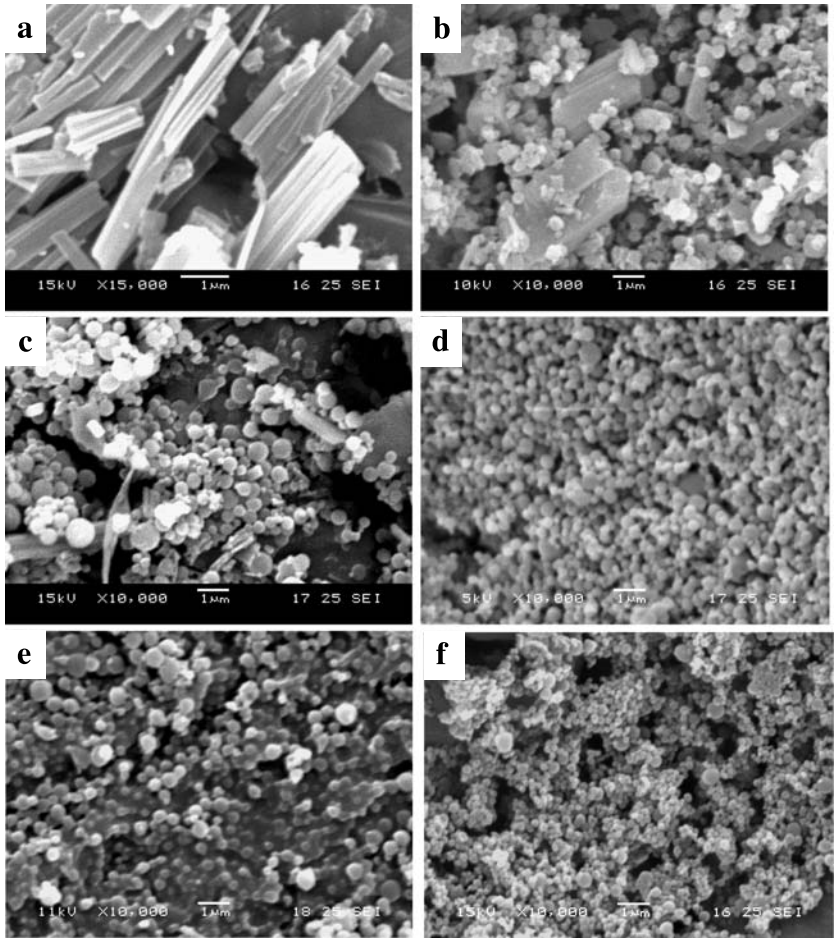

Fig. 2. SEM pictures. (a) Pure paclitaxel; (b) 30% paclitaxel-loaded PLGA nanoparticles; (c) 20% paclitaxel-loaded PLGA nanoparticles; (d) 10% paclitaxel-loaded PLGA nanoparticles; (e) 5% paclitaxel-loaded PLGA nanoparticles; (f) blank PLGA nanoparticles.

The X-ray patterns of pure paclitaxel and different drug-loading PLGA particles are shown in Fig. 4. It was observed that a small peak around 6° 2θ could appear in higher drug-loading PLGA nanoparticles (30 and 20%), a characteristic peak of pure paclitaxel. This finding suggested that some amount of drug could not be encapsulated in the polymer matrix and kept a crystalline form when the drug loadings were 20 and 30%. The small peak around 6° 2θ could not be found when drug loading was less than 10%. This indicated that no crystalline drug was detected, in accordance with DSC results of paclitaxel-loaded PLGA nanoparticles.

Drug Loading and Encapsulation Efficiency

It was observed from Table I that drug encapsulation efficiencies of paclitaxel-loaded PLGA and PLA nanoparticles were 58.9 and 57.9%, respectively. This suggested that PLGA and PLA polymer could have similar capability to encapsulate paclitaxel using a direct dialysis method when drug loading was around 10%. However, the encapsulation efficiency of paclitaxel-loaded PLGA nanoparticles was 69.0% when the drug loading was reduced to about 5% (see sample S5, Table I). This suggested that the encapsulation efficiency could increase with decreasing drug loadings. From Table I, it was seen that the encapsulation efficiency of the sample with vitamin E TPGS as an additive (75.9%) was higher than that of the sample without additives (69.0%), although their drug loadings were similar. This indicated that vitamin E TPGS as an additive could enhance the capability of drug encapsulation in the fabrication process. Therefore, the highest encapsulation efficiency (90.1%) in this study was achieved under the conditions of combined low drug loading (2%) and use of vitamin E TPGS.

Zeta Potential Analysis

Zeta potential is a useful indicator of surface charge property and can be employed as an index to the stability of the nanoparticles. In most circumstances, the higher the absolute value of the zeta potential of the particles, the larger the amount of charge on their surface. These might result in stronger repellent interactions among the particles, and hence, higher stability of the particles is achieved. It was observed that PLGA and PLA nanoparticles fabricated in this study show negative surface charge (about −20 mV) on the surface. The zeta potential of paclitaxel-loaded PLGA

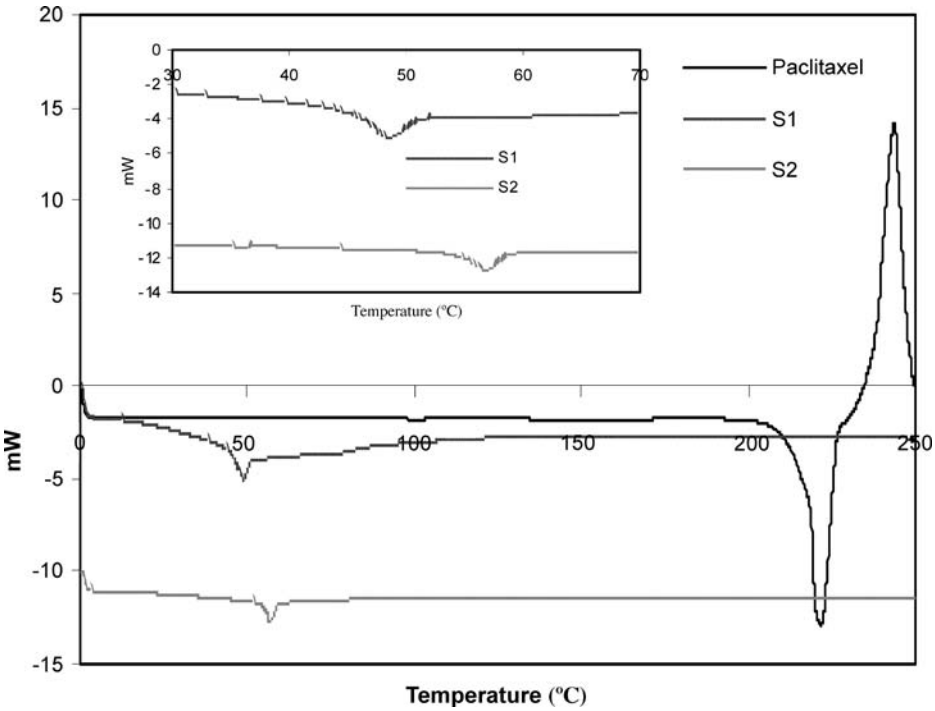

Fig. 3. Differential scanning calorimetry thermogram. S1: Paclitaxel-loaded PLA nanoparticles; S2: paclitaxel-loaded PLGA nanoparticles. Inserted chart is the enlargement of the part that indicates that the T_g of the polymer changes little after drug encapsulation.

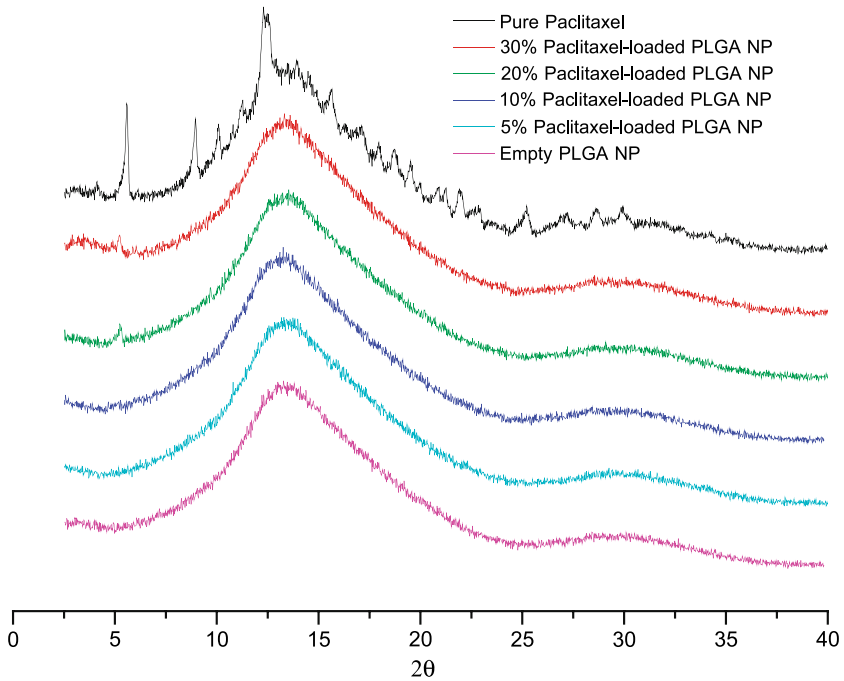

Fig. 4. X-ray diffractometry pattern. Black line: pure paclitaxel; red line: 30% drug-loading paclitaxel-loaded PLGA nanoparticles; green line: 20% drug-loading paclitaxel-loaded PLGA nanoparticles; dark blue line: 10% drug-loading paclitaxel-loaded PLGA nanoparticles; light blue line: 5% drug-loading paclitaxel-loaded PLGA nanoparticles; pink line: blank PLGA nanoparticles.

with vitamin E TPGS as an additive was similar with the sample without vitamin E, although vitamin E TPGS as a surfactant in the fabrication process could affect the surface properties of the nanoparticles by adhering on the surface of the nanoparticles. The negative zeta potential values imply negative charge on the surface and may be attributed to the presence of ionized carboxyl groups on the particle surface (27). Zeta potential of fluorescence-loaded nanoparticles (−40 mV) seemed to be more negative than that of paclitaxel-loaded particles. Therefore, to enhance the particle cellular uptake, the surface of particles might be modified by positively charged surface functional groups (28).

In Vitro Release Profile

The release curves for PLGA and PLA nanoparticles are shown in Fig. 5. High initial burst was attributed to the immediate dissolution and release of paclitaxel adhered on the surface and located near the surface of the nanoparticles. From Fig. 5, it was observed that paclitaxel may release faster from PLA nanoparticles than from PLGA nanoparticles. This could be due to different properties between PLA and PLGA polymers. The release profile can be optimized by modulating a surfactant in controlling the release profile (29,30). To realize this purpose, vitamin E TPGS (a natural emulsifier) was used as an additive in the fabrication process to tailor the release rate. It is seen from Fig. 5 that the release rate of the sample with vitamin E TPGS was higher than that without additives under similar drug loadings. The release rate of high drug-loading sample seemed to be slightly higher than that of low drug-loading sample. Because the degradation time scale of polymer is about 1–2 months, the release by polymer matrix erosion was not significant during this release period.

Particle Cellular Uptake

Particles labeled with fluorescent dyes are frequently used to study cellular uptake quantitatively by microplate reader and flow cytometry (31,32). Several measures have been taken on qualitative uptake studies using confocal microscope (33–39). Particle cellular uptake could be affected by many factors, such as particle size (40–42), different cell lines and cell densities (42), different compositions of the particles (41), surface properties (surface hydrophobic/hydrophilic balance, surface charge, zeta potential) (28,41), temperature (31), etc. Residual PVA on the particle surface also affects cellular uptake (43). Because the nanoparticles were fabricated by direct dialysis, no residual PVA was on the particle surface.

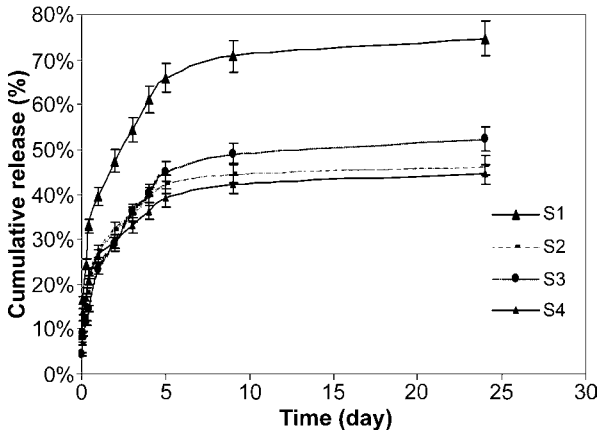

Fig. 5. Paclitaxel release curve. S1: Paclitaxel (5.7%)-loaded PLA nanoparticles; S2: paclitaxel (5.7%)-loaded PLGA nanoparticles; S3: paclitaxel (4.2%)-loaded PLGA nanoparticles with vitamin E TPGS as an additive; S4: paclitaxel (2%)-loaded PLGA nanoparticles with vitamin E TPGS as an additive. Each data point shown is the average of three samples.

Based on an earlier study, less than 0.6% of the incorporated dye could leach out from the nanoparticles over 48 h under *in vitro* sink conditions (44). Nanoparticles loaded with coumarin6 were characterized for the leaching of dye in two different pH buffers, suggesting the suitability of coumarin6 as a marker for nanoparticles (41,45,46). Coumarin6-labeled nanoparticles can be used to study the intracellular distribution through colocalization techniques. Using an organelle-specific dye with contrasting fluorescence, it is possible to study the colocalization of nanoparticles in the particular organelle. As a result, the intracellular fluorescence could not be due to the uptake of dye released or dissociated from nanoparticles.

The morphology of the coumarin6-loaded particles was observed by SEM as shown in Fig. 1e and f. C6 glioma cell line was used to evaluate the cellular uptake efficiency for PLGA and PLA nanoparticles. Nucleus staining was performed using propidium iodide (PI) and observed under confocal microscope using a two-channel mode. The fluorescein isothiocyanate channel was used to observe the particles, and neutral red channel was used to observe the cells. Fig. 8 shows that efficiency of particle cellular uptake could decrease with increasing particle concentration. In contrast, particle cellular uptake efficiency may increase with the increase in incubation time. PLGA nanoparticle uptake progress is shown in Fig. 6a–d at different time intervals, 1 and 2 h, respectively. To verify whether the nanoparticles are located just outside the top surface of the cells or entrapped intracellularly, confocal images for three orthogonal axes of the particle uptake process are shown in Fig. 7 (green color indicates PLGA nanoparticles). These images verify that these particles were indeed entrapped within the intracellular space. It was evident that much more particles were engulfed by cells after 2 h than after 1 h because of extended exposure.

PLA particles show similar properties and behavior with PLGA nanoparticles (shown in Fig. 6e and f). This could be explained in the following way. Endocytosis is usually considered to occur either constitutively by the continuous fluid-phase (pinocytic) pathway (less than 150 nm) or by phagocytosis, a ligand-induced process responsible for the uptake of large particles (larger than 200 nm) (47). Also, phagocytosis function was observed in C6 glioma cells *in vitro* and *in vivo* (48,49). Phagocytosis, the process by which cells engulf foreign particles (47,50), could have major contributions to the particle cellular uptake. Based on the fluorescence measurements (shown in Fig. 8), a significant fraction of the administered nanoparticles could be taken up through nonspecific phagocytosis by the cells.

Similar result was confirmed by flow cytometry experiments where coumarin6-labeled PLGA particle cellular

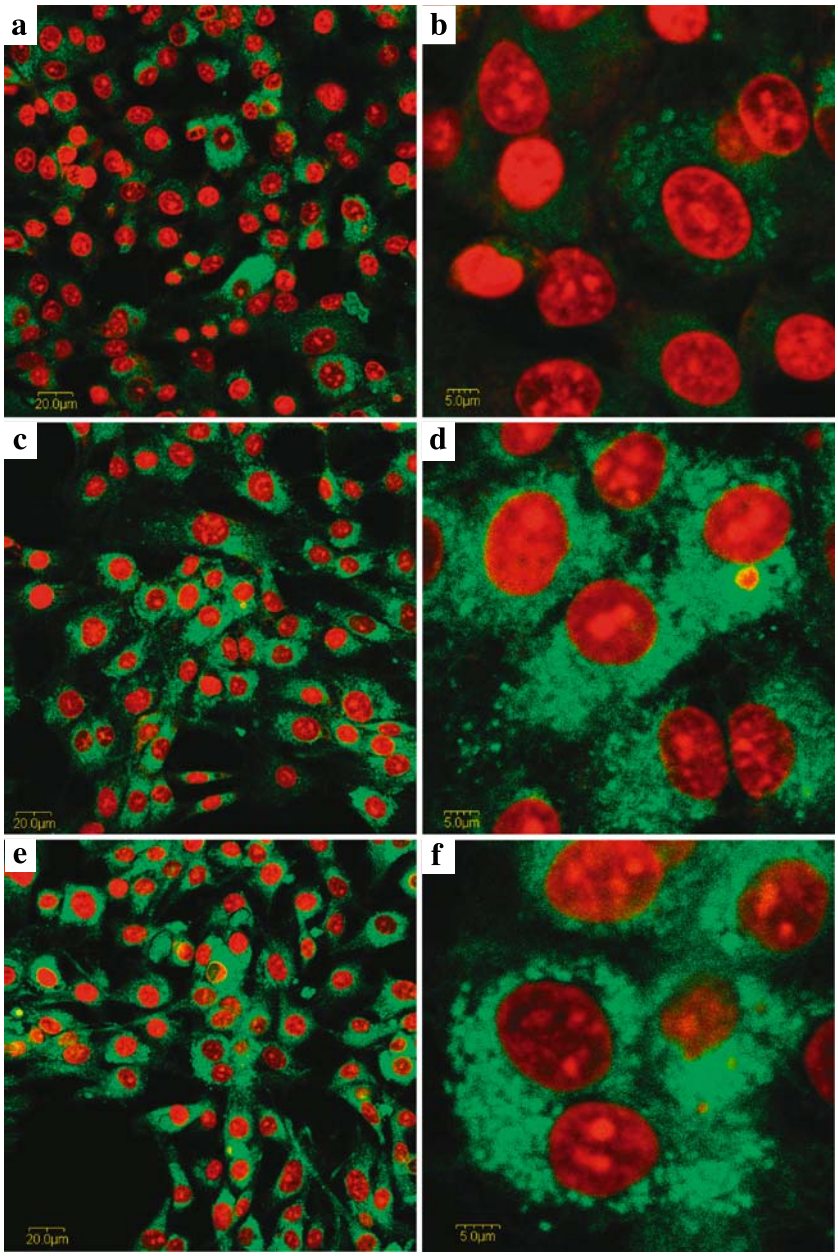

Fig. 6. Confocal fluorescence images of C6 glioma cells with coumarin6-labeled nanoparticles (200–300 nm) with different exposure times. (a, b) PLGA nanoparticle incubated for 1 h; (c, d) PLGA nanoparticle incubated for 2 h; (e, f) PLA nanoparticle incubated for 2 h. The images were collected from the fluorescein isothiocyanate channel and neutral red channel simultaneously.

uptake kinetics was quantified in the following way (Fig. 9). In Fig. 9a, "Events" indicate cell numbers. Because the nanoparticles were all loaded with fluorescent agent coumarin6, the index "fluorescence intensity" is directly proportional to the number of particles internalized by the cells. The number of cells in this figure represents the normalized number of cells (out of a fixed amount of cell samples) exhibiting a given fluorescence intensity. In contrast, Fig. 9b illustrates the median fluorescence intensity *vs.* time. This plot is computed based on the median fluorescence intensity shown in Fig. 9a.

The shifting of peak to the right along *x*-axis (Fig. 9a) suggested that the median fluorescence intensity increased with increasing incubation times (Fig. 9b). These results illustrate that coumarin6-loaded PLGA and PLA nanoparticles could penetrate through C6 glioma cell membrane and be internalized by phagocytosis process.

Cytotoxicity Test

A previous study confirmed that C6 glioma cells could grow very fast and achieve monolayer in about 5 days (51).

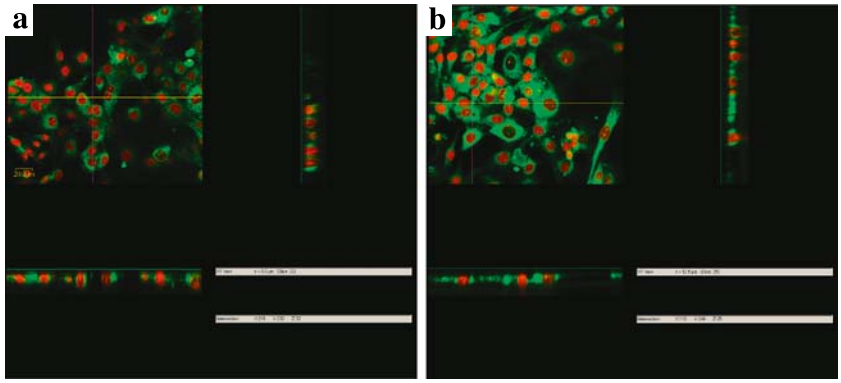

Fig. 7. Confocal images showing the cellular uptake of PLGA nanoparticles. Optical sections are displayed in three orthogonal projections [*xy*-projections (top left corner panel), *xz*-projections (down panel), and *yz*-projections (right panel)] to distinguish between extracellular and internalized nanoparticles. (a) 1 h; (b) 2 h.

The G1 phase of the cell cycle is 11–12 h in length, with a doubling time estimated to be 18 ± 2 h in asynchronous populations of C6 glioma cells (51). The nanoparticles were sterilized by γ irradiation before cytotoxicity test. γ irradiation of the samples for sterilization was performed using ^{60}Co with a total dose of 15 kGy. The cytotoxic activity of paclitaxel-loaded PLGA and PLA nanoparticles fabricated in this study (shown in Fig. 10) was evaluated by assessing cell viability using the MTT assay on C6 glioma cell line. To facilitate the basis for comparison, cells were incubated with concentrations of nanoparticles that contained the same amount of drug as that of Taxol® sample with paclitaxel concentrations of 10, 20, and 40 μg/ml, respectively. The concentrations selected were in the range corresponding to plasma levels of the drug achievable in humans (18,52). From Fig. 10, it was observed that the paclitaxel-loaded PLGA nanoparticles without additives and with vitamin E TPGS as an additive could have lower cell viability than Taxol® when the paclitaxel concentrations were 10 and 20 μg/ml, respectively. The Taxol® seemed to be more cytotoxic than paclitaxel-loaded PLGA nanoparticles when paclitaxel concentration was 40 μg/ml.

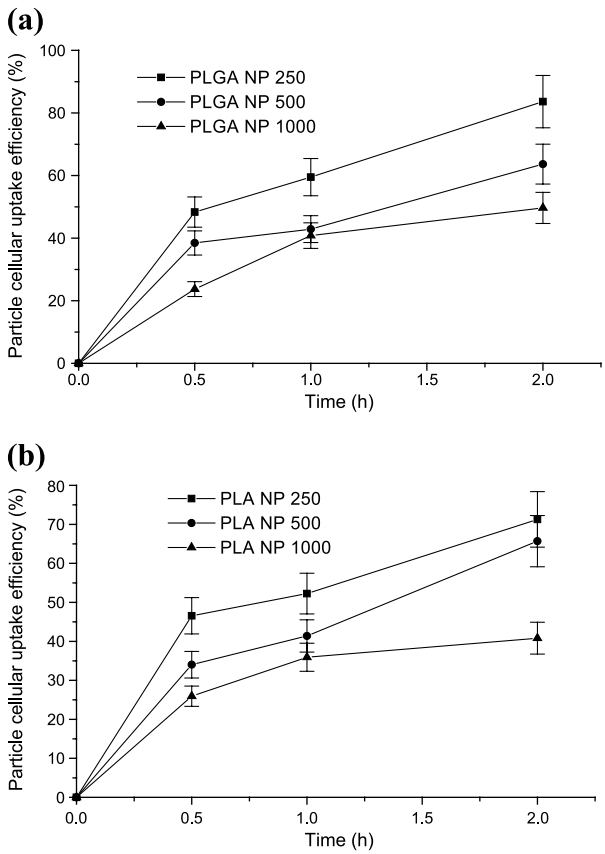

Fig. 8. The variations of particle cellular uptake efficiency with incubation time. Each data point shown is the average of four samples. (a) PLGA NP; (b) PLA NP. PLGA NP 250: concentration of coumarin6-loaded PLGA nanoparticles = 250 μg/ml; PLGA NP 500: concentration = 500 μg/ml.; PLGA NP 1000: concentration = 1000 μg/ml; PLA NP 250: concentration of coumarin6-loaded PLA nanoparticles = 250 μg/ml; PLA NP 1000: concentration = 1000 μg/ml; PLA NP 500: concentration = 500 μg/ml.

The amount of paclitaxel released from PLGA nanoparticles without additive was about 15, 16, and 18% after 1, 2, and 3 days, respectively. On the other hand, the amount of paclitaxel released from PLGA nanoparticles with vitamin E TPGS as an additive was about 14, 23, and 28% (shown in Fig. 5). According to the amount of drug released from the nanoparticles, the cytotoxicity of paclitaxel-loaded nanoparticles seemed to be higher than that of Taxol® even at the paclitaxel concentration of 40 μg/ml. No significant difference in cytotoxicity was observed between paclitaxel-loaded PLGA and PLA nanoparticles after incubation of 24 and 48 h, although the amount of paclitaxel released from PLA nanoparticles was a little higher than that from PLGA nanoparticles (data not shown). From Fig. 10, it is seen that higher concentration in the range from 10 to 40 μg/ml could more significantly reduce cell viability. The antitumor effect of paclitaxel is dependent on sustained therapeutic concentrations of the drug rather than maximal plasma concentrations because paclitaxel toxicity requires entry of cells into the M phase (4). It was reported that increasing the time of paclitaxel exposure results in increasing paclitaxel cytotoxicity (53). Because the cumulative drug release of the PLGA nanoparticles with and without additives is 18 and 28%, respectively, after 3 days, the cell viability of the samples

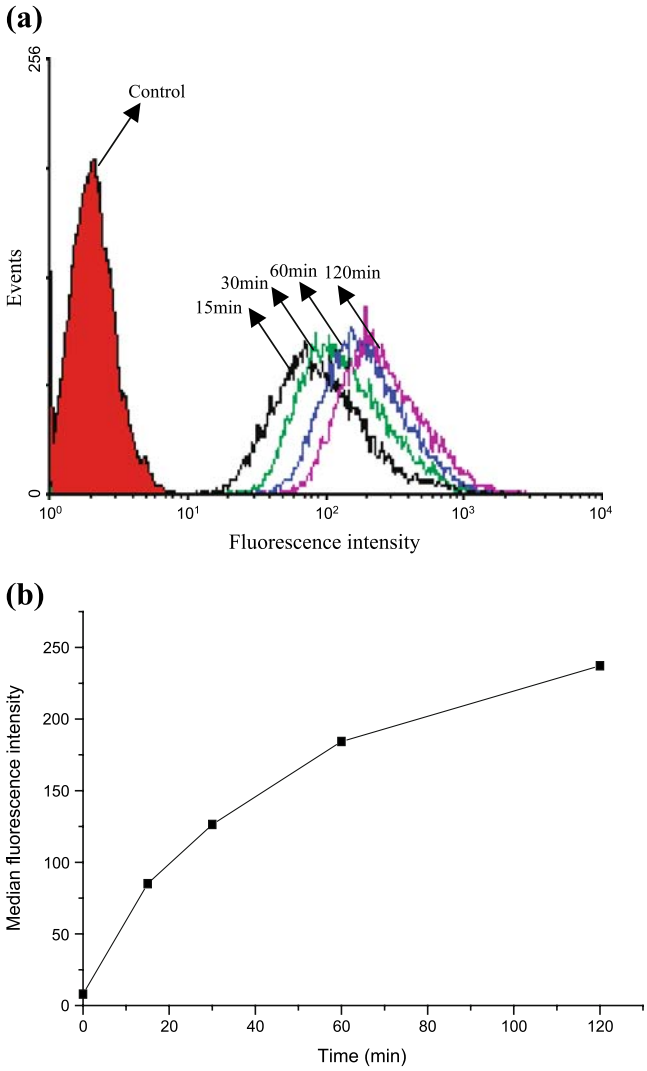

Fig. 9. Coumarin6-labeled PLGA particle cellular uptake kinetics quantified by flow cytometry. (a) Events *vs.* fluorescence intensity. "Events" indicate cell numbers. Because the nanoparticles are all loaded with fluorescent agent, the index "fluorescence intensity" is directly proportional to the number of particles internalized by the cells. The number of cells represents the normalized number of cells (out of a fixed amount of cell samples) exhibiting a given fluorescence intensity. (b) Median fluorescence intensity *vs.* time.

should be calculated by the actual amount released. Based on this normalization, the cell viability caused by vitamin E TPGS-incorporated nanoparticles was lower than that of the nanoparticles without additives after 3-day incubation. The cytotoxicity of the paclitaxel-loaded nanoparticles was dominated by the actual intracellular drug concentration caused by either particle cellular uptake or extracellular drug release from nanoparticles. Because the paclitaxel-loaded nanoparticles could have higher cytotoxicity than Taxol®, they might have advantages over Taxol® because of the sustained release properties shown in Fig. 5.

CONCLUSIONS

Paclitaxel-loaded PLGA and PLA nanoparticles were obtained successfully by direct dialysis without using an emulsifier such as PVA. The coumarin6-loaded PLGA and PLA nanoparticles could penetrate through C6 glioma cell membrane and be internalized. The results of cytotoxicity test showed that the cytotoxicity of paclitaxel-loaded nanoparticles seemed to be higher than that of Taxol® after 3 days incubation when paclitaxel concentrations were 10 and 20 μg/ml. These results could be useful for predicting possible

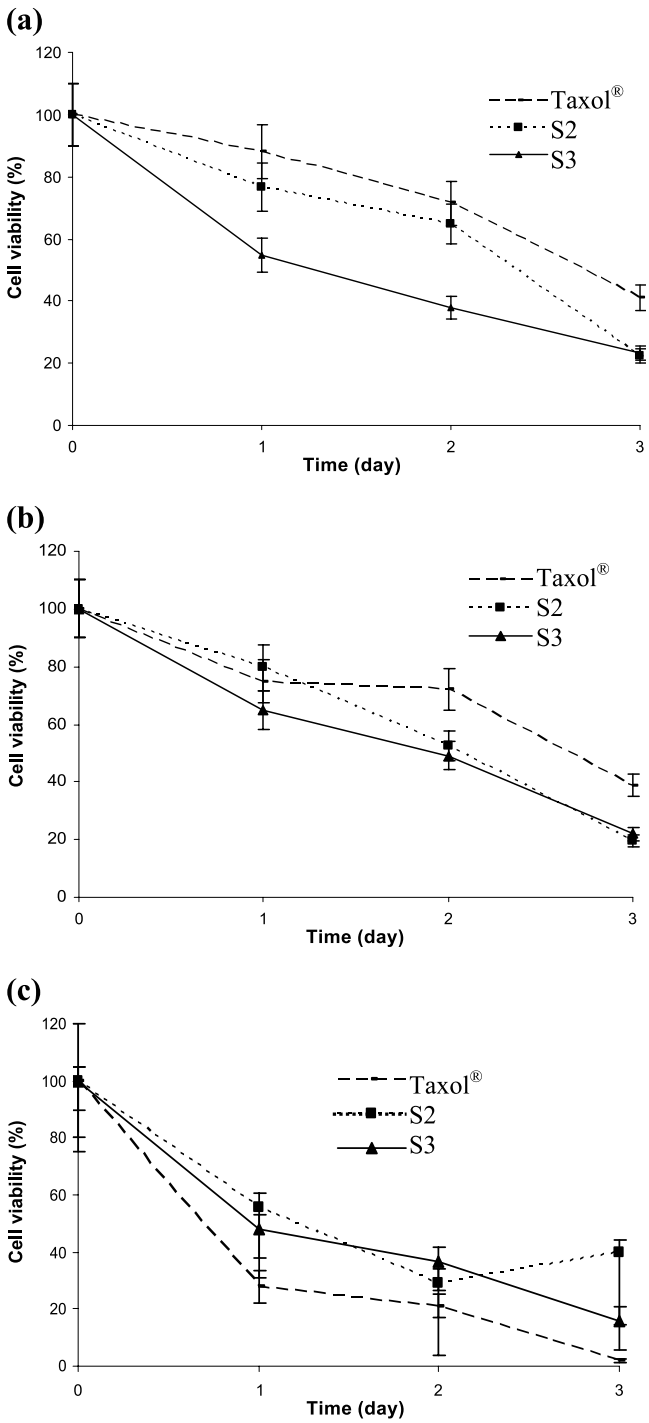

Fig. 10. Cell viability of C6 glioma cells treated with nanoparticle samples at the paclitaxel concentration of (a) 10 μg/ml, (b) 20 μg/ml, and (c) 40 μg/ml. S2: Paclitaxel-loaded PLGA nanoparticles; S3: paclitaxel-loaded PLGA nanoparticles with vitamin E TPGS as an additive. Each data point shown is the average of eight samples.

dose response of paclitaxel-loaded PLGA nanoparticles in *in vivo* test or clinical trial administration. Based on these studies, the formulations fabricated in this work could be promising for *in vivo* paclitaxel delivery. The surface of nanoparticles in this study will be modified, and animal test of the nanoparticles will be investigated by intratumoral or intravenous administration in the future work.

ACKNOWLEDGMENTS

This work is supported by the National University of Singapore under the grant number R279-000-095-112. The authors thank Professor Si-Shen Feng for many helpful discussions. They also express their appreciation to Professor Timothy Lee for providing the C6 glioma cell line samples and lab officer Kong Heng for helpful discussion and technical support on the confocal microscopy experiments.

REFERENCES

1. W. P. Mcguire, E. K. Rowinsky, N. B. Rosenshein, F. C. Grumbine, D. S. Ettinger, D. K. Armstrong, and R. C. Donehower. Taxol: a unique antineoplastic agent with significant activity in advanced ovarian epithelial neoplasms. *Ann. Intern. Med.* **111**:273–279 (1989).
2. F. A. Holmes, R. S. Walters, R. L. Theriault, A. D. Forman, L. K. Newton, M. N. Raber, A. U. Buzdar, D. K. Frye, and G. N. Hortobagyi. Phase II trials of taxol, an active drug in the treatment of metastatic breast cancer. *Natl. Cancer Inst.* **83**:1797–1805 (1991).
3. E. K. Rowinsky, M. Wright, B. Monsarrat, G. J. Lesser, and R. C. Donehower. Taxol: pharmacology, metabolism and clinical implications. *Cancer Surv.* **17**:283–301 (1993).
4. S. Gagandeep, P. M. Novikoff, M. Ott, and S. Gupta. Paclitaxel shows cytotoxic activity in human hepatocellular carcinoma cell lines. *Cancer Res.* **136**:109–118 (1999).
5. S. B. Horwitz, L. Lothstein, and J. J. Manfredi. Taxol: mechanisms of action and resistance. *Ann. N.Y. Acad. Sci.* **466**:737–744 (1986).
6. M. A. Jordan, R. J. Toso, and D. Thrower. Mechanism of mitotic block and inhibition of cell proliferation by taxol at low concentrations. *Proc. Natl. Acad. Sci. USA* **90**:9552–9556 (1993).
7. J. J. Manfredi, J. Parness, and S. B. Horwithz. Taxol binds to cellular microtubules. *J. Cell Biol.* **94**:688–696 (1982).
8. K. L. Xu and R. F. Luduena. Characterization of nuclear β_{II}-tubulin in tumor cells: a possible novel target for taxol. *Cell Motil. Cytoskelet.* **53**:39–52 (2002).
9. J. J. Zhong. Plant cell culture for production of paclitaxel and other taxanes. *J. Biosci. Bioeng.* **94**(6): 591–599 (2002).
10. O. Lehoczky, A. Bagameri, J. Udvary, and T. Pulay. Side effects of paclitaxel therapy in ovarian cancer patients. *Eur. J. Gynaecol. Oncol.* **22**(1): 81–84 (2001).
11. A. K. Singla, A. Garg, and D. Aggarwal. Paclitaxel and its formulations. *Int. J. Pharm.* **235**:179–192 (2002).
12. P. R. Lockman, R. J. Mumper, and M. A. Khan. Nanoparticle technology for drug delivery across the blood brain barrier. *Drug Dev. Ind. Pharm.* **28**(1): 1–13 (2002).
13. C. Couvreur and R. L. Treuple. Nanoparticles as microcarriers for anticancer drugs. *Adv. Drug Deliv. Rev.* **5**:209–230 (1990).
14. S. S. Feng and S. Chien. Chemotherapeutic engineering: application and further development of chemical engineering principles for chemotherapy of cancer and other diseases. *Chem. Eng. Sci.* **58**:4087–4114 (2003).
15. R. A. Jain. The manufacturing techniques of various drug loaded biodegradable poly(lactide-co-glycolide) devices. *Biomaterials* **21**:2475–2490 (2000).
16. S. S. Feng, L. Mu, B. H. Chen, and D. Pack. Polymeric nanospheres fabricated with natural emulsifiers for clinical administration of an anticancer drug paclitaxel (Taxol®). *Mater. Sci. Eng., C* **20**:85–92 (2002).
17. T. Govender, S. Stolnik, M. C. Garnett, L. Lllum, and S. S. Davis. PLGA nanoparticles prepared by nanoprecipitation: drug loading and release studies of a water soluble drug. *J. Control. Release* **57**:171–185 (1999).
18. C. Fonseca, S. Simoes, and R. Gaspar. Paclitaxel-loaded PLGA nanoparticles: preparation, physicochemical characterization and *in vitro* anti-tumoral activity. *J. Control. Release* **83**: 273–286 (2002).
19. Y. C. Dong and S. S. Feng. Methoxy poly(ethylene glycol)–poly(lactide) (MPEG-PLA) nanoparticles for controlled delivery of anticancer drugs. *Biomaterials* **25**:2843–2849 (2004).
20. K. S. Soppimath, T. M. Aminabhavi, and A. R. Kulkarni. Biodegradable polymeric nanoparticles as drug delivery devices. *J. Control. Release* **70**:1–20 (2001).
21. M. L. Hans and A. M. Lowman. Biodegradable nanoparticles for drug delivery and targeting. *Curr. Opin. Solid State Mater. Sci.* **6**:319–327 (2002).
22. F. B. Landry, D. V. Bazile, G. Spenlehauer, M. Veillard, and J. Kreuter. Release of the fluorescent marker Prodan® from poly(D,L-lactic acid) nanoparticles coated with albumin or polyvinyl alcohol in model digestive fluids (USP XXII). *J. Control. Release* **44**:227–236 (1995).
23. E. C. Lavelle, S. Sharif, N. W. Thomas, J. Holland, and S. S. Davis. The importance of gastrointestinal uptake of particles in the design of oral delivery systems. *Adv. Drug Deliv. Rev.* **18**:5–22 (1995).
24. Y. I. Jeong, J. B. Cheon, S. H. Kim, J. W. Nah, Y. M. Lee, Y. K. Sung, T. Akaike, and C. S. Cho. Clonazepam release from core-shell type nanoparticles *in vitro*. *J. Control. Release* **51**:169–178 (1998).
25. Y. I. Jeong, Y. H. Shim, C. Y. Choi, M. K. Jang, G. M. Shin, and J. W. Nah. Surfactant-free nanoparticles of poly(DL-lactide-co-glycolide) prepared with poly(L-lactide)/poly(ethylene glycol). *J. Appl. Polym. Sci.* **89**(4): 1116–1123 (2003).
26. Y. I. Jeong, C. S. Cho, S. H. Kim, K. S. Ko, S. I. Kim, Y. H. Shim, and J. W. Nah. Preparation of poly(DL-lactide-co-glycolide) nanoparticles without surfactant. *J. Appl. Polym. Sci.* **80**:2228–2236 (2001).
27. S. Stolnik, M. C. Garnett, M. C. Davis, L. Illum, M. Bousta, M. Vert, and S. S. Davis. The colloidal properties of surfactant-free biodegradable nanospheres from poly(β-malic acid-cobenzyl malate) and poly(lactic acid-co-glycolide). *Colloids Surf., A* **97**: 235–245 (1995).
28. K. A. Foster, M. Yazdanian, and K. L. Audus. Microparticulate uptake mechanism of *in-vitro* cell culture models of the respiratory epithelium. *J. Pharm. Pharmacol.* **53**:57–66 (2001).
29. L. Mu and S. S. Feng. Vitamin E TPGS used as emulsifier in the solvent evaporation/extraction technique for fabrication of polymeric nanospheres for controlled release of paclitaxel (Taxol®). *J. Control. Release* **80**:129–144 (2002).
30. S. S. Feng and G. F. Huang. Effect of emulsifiers on the controlled release of paclitaxel from nanospheres of biodegradable polymers. *J. Control. Release* **1**:53–69 (2001).
31. H. Suh, B. Jeong, F. Liu, and S. W. Kim. Cellular uptake study of biodegradable nanoparticles in vascular smooth muscle cells. *Pharm. Res.* **15**(9): 1495–1498 (1998).
32. I. Kolleck, H. Wissel, and F. Guthmann. HDL-Holoparticle uptake by alveolar type Π cells effect of vitamin E status. *Am. J. Respir. Cell Mol. Biol.* **27**:57–63 (2002).
33. P. Peter, R. R. Barbara, L. Peter, W. A. Heidi, E. Walter, and P. M. Hans. Transfer of lipophilic markers from PLGA and polystyrene nanoparticles to Caco-2 monolayers mimics particle uptake. *Pharm. Res.* **19**(5): 595–601 (2002).
34. M. E. Christine, L. Deborah, R. Robinson, C. Coester, G. S. Kwon, and J. Samuel. Analysis of poly(D,L-lactic-co-glycolic acid) nanosphere uptake by human dendritic cells and macrophages *in vitro*. *Pharm. Res.* **19**(10): 1480–1487 (2002).
35. J. S. Chawla and M. M. Amiji. Cellular uptake and concentrations of tamoxifen upon administration in poly (ε-caprolactone) nanoparticles. *AAPS PharmSci* **5**(1): 1–7 (2003).
36. Y. Mo and L. Y. Lim. Mechanic study of the uptake of wheat germ agglutinin-conjugated PLGA nanoparticles by A549 cells. *J. Pharm. Sci.* **93**:20–28 (2004).

37. G. Borchard, K. L. Audus, F. Shi, and J. Kreuter. Uptake of surfactant-coated poly(methyl methacrylate)-nanoparticles by bovine brain microvessel endothelial cell monolayers. *Int. J. Pharm.* **110**:29–35 (1994).
38. A. E. Gulyaev, S. E. Gelperina, I. N. Skidan, A. S. Antropov, G. Y. Kivman, and J. Kreuter. Significant transport of doxorubicin into the brain with polysorbate 80-coated nanoparticles. *Pharm. Res.* **16**:1564–1569 (1999).
39. P. Ramge, R. E. Unger, J. B. Oltrogge, D. Begley, H. V. Briesen, and J. Kreuter. Polysorbate-80 coating enhances uptake of polybutylcyanoacrylate (PBCA)-nanoparticles by human, bovine and murine primary brain capillary endothelial cells. *Eur. J. Neurol.* **12**:1935–1940 (2000).
40. M. P. Desai, V. Labhastetwar, G. L. Amidon, and R. J. Levy. Gastrointestinal uptake of biodegradable microparticles: effect of particle size. *Pharm. Res.* **13**:1838–1845 (1996).
41. T. Jung, W. Kamm, A. Breitenbach, E. Kaiserling, J. X. Xiao, and T. Kissel. Biodegradable nanoparticles for oral delivery of peptides: is there a role for polymers to affect mucosal uptake? *Eur. J. Pharm. Biopharm.* **50**:147–160 (2000).
42. W. Zauner, N. A. Farrow, and A. M. R. Hainess. *In vitro* uptake of polystyrene microspheres: effect of particle size, cell line and cell density. *J. Control. Release* **71**:39–51 (2001).
43. S. K. Sahoo, J. Panyam, S. Prabha, and V. Labhasetwar. Residual polyvinyl alcohol associated with poly(D,L-lactide-co-glycolide) nanoparticles affects their physical properties and cellular uptake. *J. Control. Res.* **82**:105–114 (2002).
44. M. P. Desai, V. Labhasetwar, E. Walter, R. J. Levy, and G. L. Amidon. The mechanism of uptake of biodegradable microparticles in Caco-2 cells is size dependent. *Pharm. Res.* **14**(11): 1568–1573 (1997).
45. J. Davda and V. Labhasetwar. Characterization of nanoparticles uptake by endothelial cells. *Int. J. Pharm.* **233**:51–59 (2002).
46. J. Panyam, S. K. Sahoo, S. Prabha, T. Bargar, and V. Labhasetwar. Fluorescence and electron microscopy probes for cellular and tissue uptake of poly(D,L-lactide-co-glycolide) nanoparticles. *Int. J. Pharm.* **262**:1–11 (2003).
47. A. Watts and M. Marsh. Endocytosis: what goes in and how? *J. Cell Sci.* **103**:1–8 (1992).
48. W. Noske, H. Lentzen, K. Lange, and K. Keller. Phagocytotic activity of glial cells in culture. *Exp. Cell Res.* **142**:437–445 (1982).
49. C. Zimmer, R. Weissleder, K. Poss, A. Bogdanova, S. C. Wright, and W. S. Enochs. MR imaging of phagocytosis in experimental gliomas. *Radiology* **197**:533–538 (1995).
50. M. Desjardins and G. Griffiths. Phagocytosis: latex leads the way. *Curr. Opin. Cell Biol.* **15**:498–503 (2003).
51. M. L. Martin and C. M. Regan. Transient heat shock in mid-G1-phase of the C6 glioma cell cycle impairs entry into S-phase. *Toxicol. Lett.* **59**:197–202 (1991).
52. E. Raymond, A. Hanauske, and S. Faivre et al. Effects of prolonged *versus* short-term exposure paclitaxel (Taxol®) on human tumor colony-forming units. *Anti-Cancer Drugs* **8**(4): 379–385 (1997).
53. J. E. Liebmann, J. A. Cook, C. Lipschultz, D. Teague, J. Fisher, and J. B. Mitchell. Cytotoxic studies of paclitaxel (Taxol®) in human tumour cell lines. *Br. J. Cancer* **68**:1104–1109 (1993).